High Resistivity Lipid Bilayers Assembled on Polyelectrolyte Multilayer Cushions: An Impedance Study

Eleftheria Diamanti,[†] Danijela Gregurec,[†] María José Rodríguez-Presa,[‡] Claudio A. Gervasi,*[,‡,§] Omar Azzaroni,*[,‡] and Sergio E. Moya*[,†]

[†]Soft Matter Nanotechnology Group, CIC biomaGUNE, Paseo Miramón 182 C, 20009 San Sebastián, Guipúzcoa, Spain
[‡]Instituto de Investigaciones, Fisicoquímicas Teóricas y Aplicadas (INIFTA), Departamento de Química, Facultad de Ciencias Exactas, Universidad Nacional de la Plata, CONICET, Sucursal 4-C.C.16, 1900 La Plata, Argentina
[§]Area Electroquímica, Facultad de Ingeniería, Universidad Nacional de La Plata, calle 1 y 47, 1900 La Plata, Argentina

S *Supporting Information*

ABSTRACT: Supported membranes on top of polymer cushions are interesting models of biomembranes as cell membranes are supported on a polymer network of proteins and sugars. In this work lipid vesicles formed by a mixture of 30% 1,2-dioleoyl-*sn*-glycero-3-phosphocholine (DOPC) and 70% 1,2-dioleoyl-*sn*-glycero-3-phospho-L-serine (DOPS) are assembled on top of a polyelectrolyte multilayer (PEM) cushion of poly(allylamine hydrochloride) (PAH) and poly-(styrene sodium sulfonate) (PSS). The assembly results in the formation of a bilayer on top of the PEM as proven by means of the quartz crystal microbalance with dissipation technique (QCM-D) and by cryo-transmission electron microscopy (cryo-TEM). The electrical properties of the bilayer are

studied by electrochemical impedance spectroscopy (EIS). The bilayer supported on the PEMs shows a high resistance, on the order of 10^7 Ω cm^2, which is indicative of a continuous, dense bilayer. Such resistance is comparable with the resistance of black lipid membranes. This is the first time that such values are obtained for lipid bilayers supported on PEMs. The assembly of polyelectrolytes on top of a lipid bilayer decreases the resistance of the bilayer up to 2 orders of magnitude. The assembly of the polyelectrolytes on the lipids induces defects or pores in the bilayer which in turn prompts a decrease in the measured resistance.
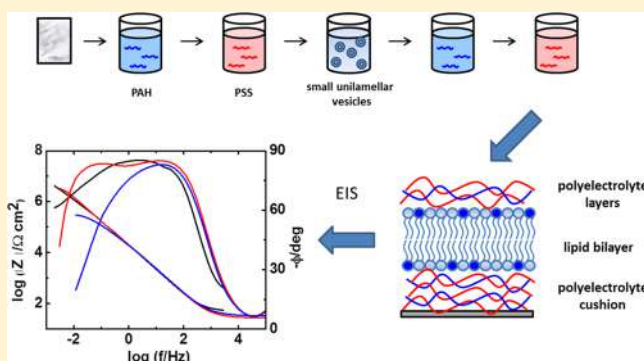
INTRODUCTION

Lipid layers assembled on top of substrates of different nature represent a subject of research on their own.[1,2] The so-called supported lipid membranes have been extensively used as models for biophysical studies of cell membranes[3−5] and as a means to modify surfaces to improve their biocompatibility[6] or to integrate sensing elements. Besides the lipid components, the supported membranes may include membrane proteins, receptors, channels, and nonnatural molecules increasing functionality.[7−9] As a model for cell membranes, the coupling of lipid layers with a supporting interface has been very useful for the investigation of issues related to membrane transport, the spatial arrangement of lipids and biomolecules in the two lipid monolayers, the electrical properties of membranes, specific receptor ligand interaction, etc.[10−12] Supported membranes have been integrated in multiple devices, especially for sensing, where the membrane is used to provide a biological interface and a point of anchorage of enzymes or receptors, which will fulfill, for example, a sensing function.[13,14] Significant research has been conducted on membranes supported on planar and hard substrates such as TiO$_2$ or Au.[15,16] Comparatively less work has been dedicated to membranes

supported on polymeric surfaces, which are an interesting model system, as biological membranes are supported on top of a cushion of biopolymers, the glycocalix, or the cell wall.[11] Of particular interest in this regard is the work of Möhwald et al. involving the assembly of lipid membranes on top of polyelectrolyte (PE) multilayers fabricated by the layer-by-layer (LbL) technique.[17] The LbL is based on the alternating assembly of polyelectrolytes of opposite charge to form a thin film.[18,19] The lipid layers on PE multilayers have been used to control the permeability of PE capsules.[20] In particular, it has been shown that polyelectrolyte multilayers exhibit a decrease in conductivity after lipid assembly.[21,22] In addition, the conditions for the assembly of a lipid bilayer on top of polyelectrolyte multilayers requires a balance between zwitterionic and charged lipids, which is achieved when the proportion of charged lipids is more than 50 mol % of the total lipid content as shown by Fischlechner et al.[23]
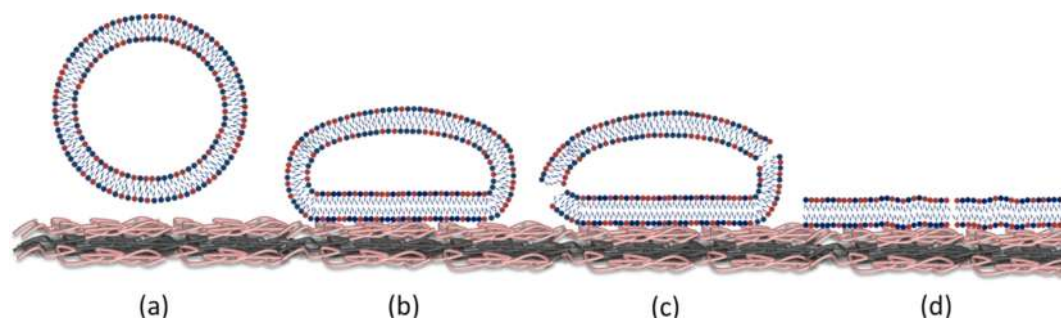
Figure 1. Schematic illustration of the mechanism of formation of a lipid bilayer on top of polyelectrolyte multilayer film. (a) Vesicle attraction to the PEM surface, (b) vesicle adsorption and deformation, (c) vesicle rupture, and (d) fusion of neighboring lipid patches and subsequent lipid bilayer formation.

Electrochemical impedance spectroscopy (EIS) studies have been conducted by Knoll et al. on lipid layers formed from negatively charged dimyristoyl-L-α-phosphatidylglycerol (DMPG) and the zwitterionic dimyristoyl-L-α-phosphatidyl-choline (DMPC) unilamellar vesicles assembled on PE multilayer supports.[24] These impedance studies showed the successful formation of a lipid bilayer on microcontact printed self-assembled microlayers (SAMs).[25] Electrical resistivity of lipid bilayers of anionic dioleoylphosphatidic acid (DOPA) and the zwitterionic dimyristoylphosphatidylcholine (DMPC) assembled on a PE multilayer support has been also studied in the past by means of EIS in the 0.1 Hz−30 kHz frequency range[17] revealing that the polymer support might participate in the formation of conducting defects.

Since the EIS studies conducted so far with lipid layers deposited on polyelectrolyte cushions have only been performed in conditions where the assembly does not lead to a bilayer but to non fully fused vesicles or multilayers of lipid vesicles deposited on the multilayers, the electrochemical properties of a lipid bilayer interacting with PE multilayers remain a largely unexplored issue. This subject is intrinsically interesting and worthy of study in its own right, as it would be important to determine whether the assembled lipid bilayer on top of the PE cushion can display resistance and capacity values close to those of a biomembrane when they are forming a bilayer. Up to now most works on lipids assembled on polyelectrolyte multilayers (PEMs) have revealed that this type of interfacial architecture exhibits much lower resistivity and capacitance values[17,24,26] as compared to the ones obtained in black membranes.[27−29] We hypothesize that these differences arise from the fact that in previous works the deposited lipids are not forming a bilayer but they are assembled as nonfused vesicles, with defects and free space between vesicles, which are responsible for the high conductance of the lipid assemblies. Only when a continuous and dense lipid bilayer is formed on the PEMs a high resistivity can be expected. It is also of fundamental interest to address the effect of the lipid composition on the conductance and capacitance of the bilayer, i.e., the ratio of charged to zwitterionic lipids, the type of lipid, or the presence of cholesterol. Another aspect that has not been studied is the impact of PE layers deposited on top of the upper leaflet of a lipid bilayer. The bilayer would be then sandwiched between PE layers. The polyelectrolytes on top could generate defects on the membranes or the reorganization of the lipids around the charged moieties of the polyelectrolyte. A sandwiched bilayer between polyelectrolytes could have interesting applications in the design of devices or sensors.

To address these issues, we have conducted EIS studies on lipid bilayers supported on polyelectrolyte multilayers of poly(allylamine hydrochloride) (PAH) and poly(styrene sodium sulfonate) (PSS) assembled by the layer-by-layer technique on planar substrates (Figure 1). Lipid vesicles formed by a mixture of 1,2-dioleoyl-sn-glycero-3-phosphocho-line (DOPC) and 1,2-dioleoyl-sn-glycero-3-phospho-L-serine (DOPS) were assembled into a bilayer. We have shown that, using vesicles based on these lipids, a bilayer is formed on top of PAH/PSS PEMs. Bilayer formation was confirmed by means of the quartz crystal microbalance with dissipation technique (QCM-D) and by cryo-transmission electron microscopy (cryo-TEM). The impact of the assembly of PE layers on top of the lipid layers was also studied by QCM-D. The electrical properties of the lipid bilayers were characterized by electro-chemical spectroscopy.

■ MATERIALS AND METHODS

Poly(allylamine hydrochloride) (PAH, M_w 15 kDa), poly-(styrenesulfonate sodium salt) (PSS, M_w 70 kDa), sodium 3-mercapto-1-propanesulfonate (MPS, M_w 178.21 g/mol), and choles-terol (M_w 386.65 g/mol) were purchased from Sigma-Aldrich. Phospholipids 1,2-dioleoyl-sn-glycero-3-phosphocholine (DOPC, 10 mg mL^{-1} in chloroform) and 1,2-dioleoyl-sn-glycero-3-phospho-L-serine (DOPS, sodium salt, 10 mg mL^{-1} in chloroform) were obtained from Avanti Polar Lipids, Inc. SiO$_2$ particles with a diameter of 200 nm were purchased from Attendbio. Phosphate-buffered saline (PBS), potassium chloride (KCl), sodium chloride (NaCl), and chloroform (anhydrous, >99%) were purchased from Sigma-Aldrich. Ethanol (99.9% HPLC) was obtained from Scharlau S.A.

Polyelectrolyte Multilayer Supports. Polyelectrolyte multilayer cushions were assembled using the LbL. Eleven layers of positively charged PAH and negatively charged PSS were assembled from solutions with a polyelectrolyte concentration of 1 mg mL^{-1} in 0.5 M NaCl. For each layer deposition, surfaces were incubated during 15 min at room temperature in the polyelectrolyte solution. Each step of polyelectrolyte deposition was followed by a washing step with 0.5 M NaCl. The multilayer film was deposited, following the same procedure, on top of diverse surfaces depending on the study; quartz crystals with a fundamental frequency of 5 MHz coated with SiO$_2$ (Q-Sense) were used for the QCM-D measurements, gold surfaces coated with a self-assembled monolayer of MPS in ethanol 0.1 M were used for the EIS measurements, and SiO$_2$ nanoparticles were coated with a polyelectrolyte multilayer for the cryo-TEM measurements.

Liposome Preparation and Characterization. The procedure for the preparation of the vesicles formed by mixtures of DOPC, DOPS, and cholesterol is as follows. First, lipid stock solutions in chloroform (10 mg mL^{-1}) were mixed together at molar ratios (DOPC:DOPS) of 30:70 and 30:70 and 30% cholesterol, respectively. The chloroform was evaporated with an argon stream and followed by at least 1 h incubation under vacuum in order to remove any
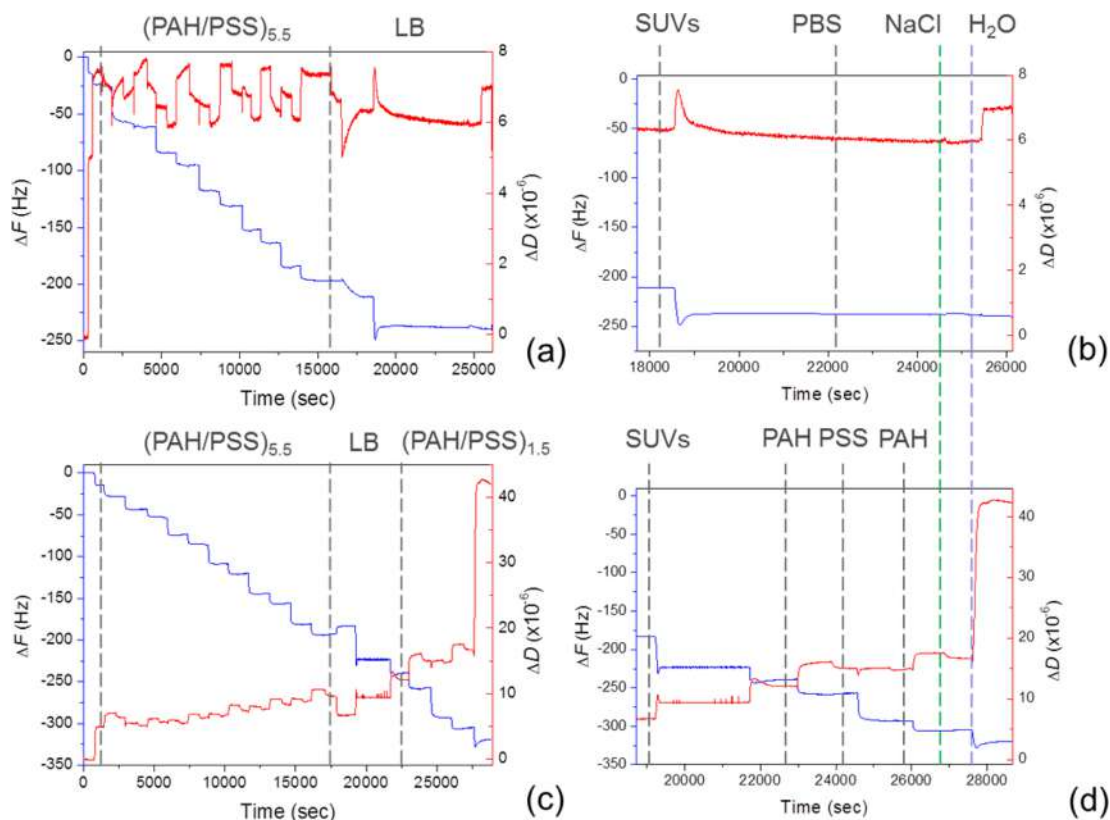
Figure 2. Changes in frequency (curve in blue) and dissipation (curve in red) of SiO$_2$-coated QCM-D crystals (a) during the assembly of 11 layers of PAH/PSS and injection of 30:70 DOPC:DOPS vesicles. The area between the dashed lines corresponds to the PEM assembly until the moment of injection of the vesicles. (b) Magnification of the area of the curve corresponds to the lipid bilayer formation. Dashed lines demonstrate the moments of injection of mentioned solutions. (c) Assembly of 11 layers of PAH/PSS, injection of 30:70 DOPC:DOPS vesicles and addition of three layers of PAH/PSS. Dashed lines indicate the areas of PEM and lipid bilayer assembly. (d) Magnification of the area of the curve that corresponds to the lipid bilayer formation and the addition of three layers. Dashed lines demonstrate the moments of injection of mentioned solutions.

chloroform trace. The resulting lipid film was rehydrated with PBS (10 mM), forming large multilamellar vesicles (MLVs) which were extruded through a 50 nm polycarbonate membrane forming small unilamellar vesicles (SUVs).

In order to determine the size and charge of the prepared vesicles, dynamic light scattering (DLS) and ζ-potential measurements were conducted. ^{1}H NMR was used to reveal the exact composition of both DOPC and DOPS in the lipid mixture. The chloroform from the lipid mixture was first evaporated, and then it was redissolved in CDCl$_3$ at a concentration of 0.6 mg mL^{-1}.

QCM-D Measurements. The multilayer assembly of PAH and PSS was followed by QCM-D (Q-Sense E4). Before the injection of the polyelectrolyte solution, the surfaces were rinsed in Milli-Q water for 10 min and then in 0.5 M NaCl for 10 min under continuous flow in the chamber. Each polyelectrolyte solution was injected during 10 min through the chamber until a stable frequency value was achieved. Each deposition was followed by 10 min of rinsing with 0.5 M NaCl (under continuous flow). In all the multilayers the capping layer was positively charged PAH (11th layer). Then, the chamber was filled with PBS, and the dispersion of SUVs in PBS (0.1 mg mL^{-1}) was injected. When the frequency reached a stable value, the quartz sensor was rinsed with PBS to remove nonadsorbed vesicles. Finally, the membrane was rinsed with Milli-Q water.

Cryo-TEM measurements. Lipid bilayer morphology was characterized by cryo-TEM using a JEOL JEM-2200FS field emission TEM with a digital camera and an in-column energy filter (Omega filter). SiO$_2$ particles were coated with 11 layers of PAH and PSS, with PAH always being the last deposited layer; thus the SUVs were incubated with the PEM coated SiO$_2$ particles in PBS solution at a molar ratio of 3:1 respectively. Before vitrification the SUVs were incubated for 1/2 h with the polyelectrolyte coated SiO$_2$ particles in

PBS. Afterward, the specimen was deposited on QUANTIFOIL grids, Holey Carbon Films (shape R2/2). The suspended sample in aqueous solution was then rapidly frozen in liquid ethane and cooled to liquid nitrogen temperature; the whole process was performed on a Vitrobot setup (FEI).

Electrochemical Impedance Spectroscopy Measurements. A general-purpose three-electrode electrochemical cell was used to perform the impedance characterization of the lipid membrane in contact with the soft polyelectrolyte cushions. A gold surface was used as the substrate of the working electrode. The multilayer cushion and the lipid bilayer were deposited on top of the gold surface, which had been previously modified with a self-assembled monolayer of MPS. For the assembly of the thiol monolayer the gold surface was left in MPS solution overnight, resulting in a negatively charged surface. A platinum (Pt) plate served as the counter electrode. Potentials were measured with respect to a silver/silver chloride reference electrode (Ag/AgCl/saturated KCl with a potential of 0.199 V vs SHE (standard hydrogen electrode)). Measurements were conducted in 0.1 M KCl electrolyte solution.

■ RESULTS AND DISCUSSION

Lipid Vesicle Characterization. First, the conditions for obtaining a bilayer on the multilayers were revised. Since the concentration of lipids in chloroform solutions may differ from the information provided by the supplier, it is necessary to determine the exact molar ratio of charged to zwitterionic lipids of the depositing vesicles. ^{1}H NMR measurements of the lipid mixtures were conducted in deuterated chloroform. For the bilayer deposition the chosen composition of the vesicles was 30:70 DOPC:DOPS. ^{1}H NMR revealed that the theoretical
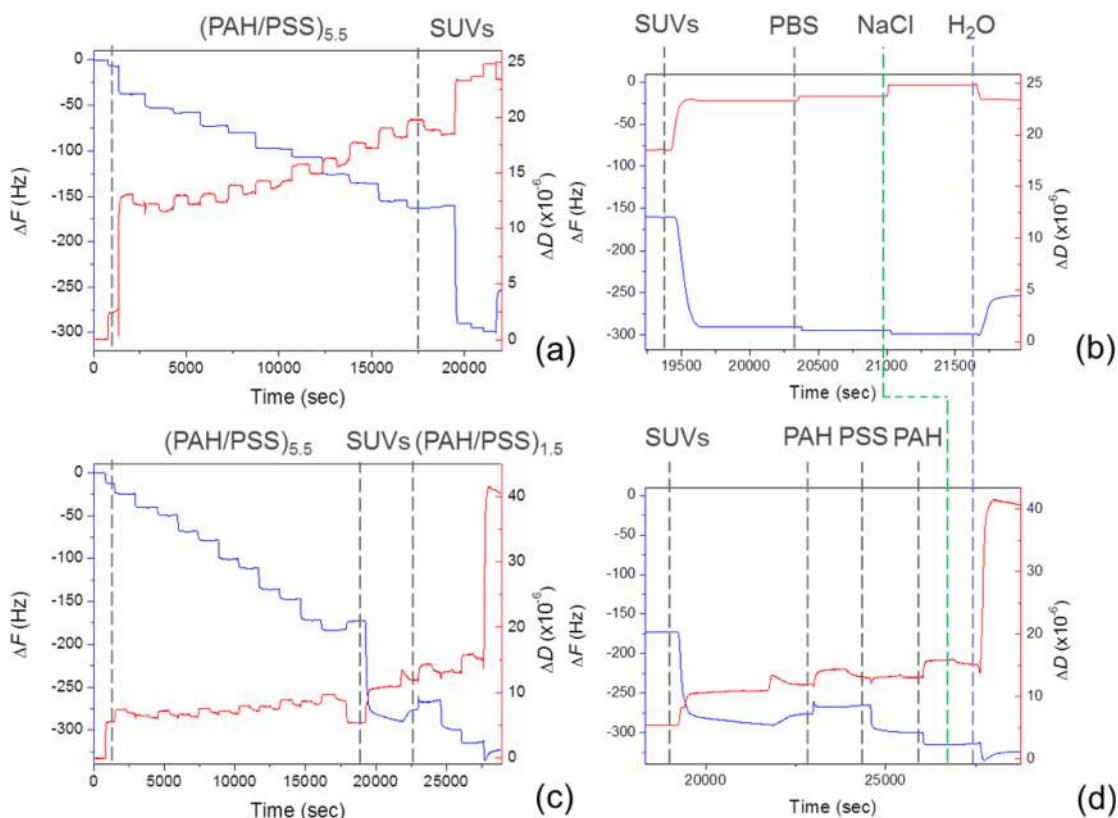
Figure 3. Changes in frequency (curve in blue) and dissipation (curve in red) of SiO$_2$-coated QCM-D crystals (a) during the assembly of 11 layers of PAH/PSS and injection of 30:70 DOPC:DOPS vesicles with 30% Chol. The area between the dashed lines corresponds to the PEM assembly until the moment of injection of the vesicles. (b) Magnification of the area of the curve corresponds to the adsorption of the SUVs containing Chol. Dashed lines demonstrate the moments of injection of mentioned solutions. (c) Assembly of 11 layers of PAH/PSS, injection of 30:70 DOPC:DOPS vesicles with 30% Chol, and addition of three layers of PAH/PSS. Dashed lines indicate the areas of PEM and SUVs containing Chol assembly. (d) Magnification of the area of the curve that corresponds to the SUVs containing Chol adsorption and the addition of three layers. Dashed lines demonstrate the moments of injection of mentioned solutions.

ratio of 30:70 DOPC:DOPS was actually present in the lipid mixture (Figure S1a in the Supporting Information).

Results from DLS measurements are illustrated in Figure S1b. Size distributions shown by intensity revealed diameters of ~79 nm for the 30:70 DOPC:DOPS composition. The diameter of the vesicles increases to ~140 nm when 30% cholesterol is added to the same lipid composition. Cholesterol molecules orient themselves in the lipid vesicles with their hydroxyl groups close to the polar head groups of the phospholipid molecules. In this position, their rigid steroid rings interact and partly immobilize the hydrocarbon chain regions closer to the polar head groups, rendering the lipid vesicle and the bilayer less deformable; thus vesicles are more difficult to extrude through the 50 nm membrane. Subsequently, by the addition of 30% cholesterol (Chol) the resulting vesicles are larger. ζ-Potential measurements of the unilamellar vesicles had, as expected, negative potential values due to the presence of the negatively charged DOPS. ζ-Potential values of −40.9 and −40.6 mV were measured for PC:PS and PC:PS:Chol, revealing close charge values for the two different lipid compositions (Figure S1b).

Evaluation of the Lipid Bilayer Formation. QCM-D measurements corroborated that the experimental conditions used for the electrochemical studies were optimal for a lipid bilayer formation using vesicles with a 30:70 ratio of PC:PS on top of 11 layers of PAH and PSS (Figure 2a). In Figure 2a typical frequency and dissipation shifts due to the formation of

a lipid bilayer can be observed. After addition of the vesicles the frequency decreases rapidly, indicating the adsorption of the vesicles onto the PEM surface. A fast increase of the frequency is detected 3 min after the injection. This increase is related to a decrease in mass, and it is a consequence of the liberation of water after the rupture of the vesicles. Finally, the frequency remains constant due to the formation of a continuous lipid bilayer with a negative surface charge that precludes further adsorption of additional vesicles from the SUV solution due to electrostatic repulsion. The total frequency change, due to the vesicle assembly, was Δf = 25.91 Hz, thus indicating the presence of a complete and stable bilayer.[1] Dissipation shows a similar behavior: it increases rapidly to decrease immediately until it remains constant. The rapid increase in dissipation is associated with the deposition of the soft vesicles on the PEM; when they rupture and fuse, they form a continuous bilayer with solidlike characteristics, which is responsible for the decrease in dissipation. By the addition of 30% cholesterol in the formulation of the vesicles (Figure 3a) the frequency decreases and remains constant, while no rapid increase is detected. The total shift was 130 Hz, a quite high value for the adsorption of vesicles. In similar experiments, when the same lipid and cholesterol compositions were deposited on top of five layers of PAH/PSS, the resulting frequency shift was 53 Hz.

The frequency values resulting from the assembly of vesicles with cholesterol, together with the absence of the jump in frequency and dissipation, hint that vesicles with cholesterol

remain unperturbed on the PEM, without fusing. However, when the same vesicles were fused on colloids coated with PEMs, we observed by means of cryo-TEM the presence of a bilayer (data not shown). The formation of a bilayer on top of PEMs is very much dependent on the proportion of charged and zwitterionic lipids. Charged lipids are fundamental for the interaction of the vesicles with the PEMs and vesicle rupture, while zwitterionic lipids seem to help in the reorganization of the vesicle to rearrange on the surface and lead to the fusion of lipid patches. The presence of cholesterol might render the vesicles too rigid to reorganize and fuse or even might restrict the vesicle rupture.

Figure 2c shows the deposition of a PAH layer on top of the bilayer of DOPC:DOPS as described previously. Frequency decreases upon deposition of the positively charged polyelectrolyte and results in a frequency shift close to 16 Hz, similar to that of the previously deposited PAH layers. Another two polyelectrolyte layers where deposited on top afterwards. For these additional layers the frequency and dissipation shifts were as expected for the deposition of a polyelectrolyte layer.

Cryo-TEM was also used as a tool to confirm the presence of the lipid bilayer on PEMs assembled on SiO_2 colloidal particles. Figure 4 displays the cryo-TEM images of SiO_2 colloids
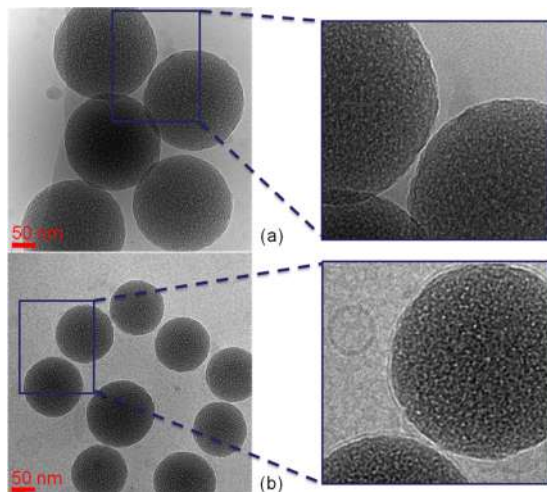
Figure 4. Cryo-TEM images of (a) SiO_2 (PAH/PSS)$_{5.5}$ and (b) SiO_2 (PAH/PSS)$_{5.5}$ particles with 30:70 DOPC:DOPS on top.

covered with 11 layers of PAH and PSS (Figure 4a) and the SiO_2 particles with a PAH/PSS PEM after coating with 30:70 DOPC:DOPS vesicles (Figure 4b). In Figure 4b we observe the assembled lipid bilayer, which forms a homogeneous layer on the PEM coated particles with a thickness of ~5 nm.

Electrochemical Characterization. The experimental impedance of the gold substrates coated with polymer cushions in the form of 5 and 11 layers of the sequence PAH/PSS are shown as Bode plots in Figure 5. The measured impedance of the PEM films clearly exhibits a single capacitive relaxation behavior that can be fitted to the impedance of an equivalent circuit containing a series connection of the electrolyte resistance R_e and an impedance element resulting from the parallel connection of a capacitor and a large resistance. For the results shown in Figure 5 the response at frequencies larger than 1 Hz resembles an ideally polarizable interface with a phase angle approaching −90°. The capacitor has a slight frequency dispersion effect, it reflects a distribution of the
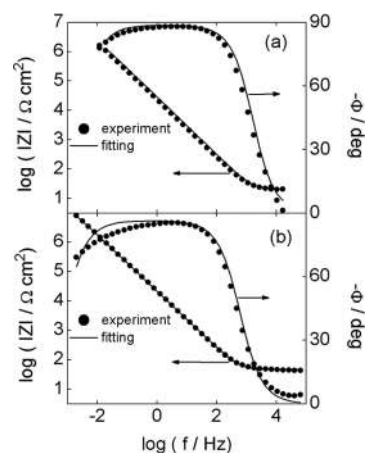
Figure 5. Bode plots for impedance spectra of multilayer cushions on gold electrodes: (a) five-layer cushion; (b) 11-layer cushion. Experimental spectra were fitted to the impedance of the equivalent circuit in Figure 6a.

interfacial capacitance due to surface inhomogeneity in the presence of the PE film, and, consequently, it is represented here by a constant phase element Q_f (see circuit in Figure 6a).
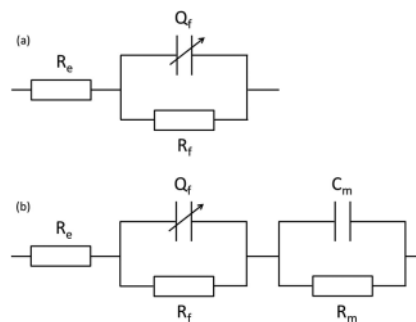
Figure 6. Equivalent circuits used to analyze experimental impedance data. For definitions of the impedance elements see text and legend for Table 1.

A resistance of the PE film R_f in parallel connection with Q_f is always considered here,[30] but in the experiments shown in Figure 6 R_f is apparently too large and it is detected for the measured frequency range $f < 1$ Hz. The exact origin of R_f as described in the literature remains controversial. In fact, R_f was related to an electron charge transfer resistance at the substrate,[31] or as described elsewhere, "some electrochemistry" is expected to take place at defect sites in the film giving rise to a shunt resistance in the equivalent circuit.[32] In this work, however, there are no electroactive species with a decomposition potential in the studied potential window. According to Guidelli and Becucci[30] a hydrophilic spacer, the polyelectrolyte multilayer in our experiments, on top of which the bilayer membrane is supported, represents, from an impedance point of view, a dielectric slab contacting the substrate, across which there is a slight ionic flux or equivalently a resistance with a value that is high, though not infinitely high. Moreover, we have shown in a previous paper that PAH/PSS films bear a constant water content irrespective of their layer number and water is mainly located at the film interface. Therefore, ion conductance is expected to take place through defects in the layers.[33]

Best-fit results of impedance data in Figure 5 are given in Table 1. Values for the exponent n are close to 1, i.e. a capacitance behavior, becoming slightly smaller when the number of layers in the hydrophilic spacer film is increased.

Table 1. Best-Fit Parameters Derived from Experimental Impedance Spectra in Figure 5 and Theoretical Impedance According to the Equivalent Circuit in Figure 6a[a]

PE cushion	R_e, Ω cm^2	Y_O, F cm^{-2} s^{n-1}	n	R_f, Ω cm^2
5 PAH/PSS layers	31.70	6.23×10^{-6}	0.97	1.02×10^7
11 PAH/PSS layers	49.40	7.90×10^{-6}	0.96	2.06×10^7

[a]The impedance of the constant phase element is $Q_f = (j\omega)^{-n}/Y_O$ with $j = \sqrt{-1}$ and $\omega = 2\pi f$ is the ac signal frequency.

Figure 6 shows the equivalent circuits used to interpret experimental impedance data for the different electrochemical interfaces. Figure 6a is the electrical analogue of an electrode coated with a PE cushion, and Figure 6b is used for determining the interfacial behavior of electrodes modified with PE layers and a lipid bilayer.

In the present study especially important parameters to derive by using EIS are the capacitance C_m and resistance R_m of the bilayer membrane. The expected values for the membrane resistance of black lipid membranes that separate two aqueous electrolytes are larger than 10 MΩ cm^2 in the absence of species that promote the formation of conducting paths for ionic transport.[27,34] The typical range for R_m values of membranes on Au surfaces as measured by impedance spectroscopy are 10^5-10^7 Ω cm^2.[35] For membranes supported on PE cushions low resistances of 2000 Ω cm^2 and capacitance values on the order of 10 μF cm^2 were reported.[17]

Figure 7a shows Bode plots of a lipid bilayer with a composition of 30:70 DOPC:DOPS and supported on a PE
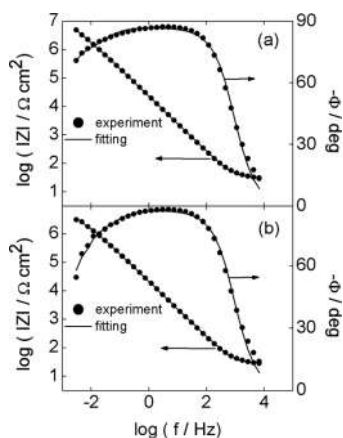
Figure 7. Bode plots for impedance spectra of lipid bilayers supported on an 11-layer PE cushion with compositions (a) of 30:70 DOPC:DOPS and (b) of 20:50:30 DOPC:DOPS:Chol. Experimental spectra were fitted to the impedance of the equivalent circuit in Figure 6b.

cushion in the form of 11 layers of PAH/PSS. Figure 7b displays Bode plots for a bilayer with a composition of 20:50:30 DOPC:DOPS:Chol on top of 11 layers of PAH/PSS. Both spectra can be satisfactorily interpreted in terms of the equivalent circuit from Figure 6b. The responses in the high-frequency region are dominated by the lipid membrane parameters R_m and C_m, while the low-frequency portions of each spectrum are related to the relaxation phenomena in the PE films ($Q_f - R_f$).[31] Best-fit results of impedance data in Figure 7 are given in Table 2.

Membrane resistances in Table 2 indicate the formation of coherent bilayers. A 30:70 DOPC:DOPS bilayer deposited on top of a PAH/PSS polyelectrolyte multilayer cushion displays a resistance of 1.89×10^7 Ω cm^2. This is a value comparable with the resistance of black lipid membranes and several orders of magnitude higher than previously reported resistances for lipids assembled on PEMs. The presence of cholesterol in the vesicles leads in our case to lower resistance, 7.69×10^6 Ω cm^2. The lower resistance in the presence of cholesterol can be a consequence of an incomplete bilayer as the QCM-D data suggested.

The membrane capacitance values measured by EIS are relatively high. Membrane capacity strongly depends on the lipid composition and conformational state (tilt angle, etc.) of the lipid chains through the resulting ratio of dielectric constant/thickness.[36] The assembly of the lipids on top of the polyelectrolyte multilayers may induce significant changes in the dielectric environment of the lipid layer in contact with the polyelectrolyte as the positively charged groups of PAH can compensate the opposite charges of DOPS and trigger reorganization of the lipids. The negatively charged lipid, DOPS, will tend to associate with the charged groups of PAH more strongly than DOPC, and this will have an impact on the distribution of DOPC and DOPS in the membrane. We can also think that, because of the interaction with PAH, the DOPS concentrated on the side of the membrane interacting with the polyelectrolyte may be higher, generating an asymmetric lipid composition. All these issues could have an impact on the membrane capacitance and explain their elevated values.

The same qualitative results were obtained with lipid bilayers supported on a five-layer PE cushion (results not shown). From a quantitative point of view R_m still exhibits unusually large values (0.5×10^7 Ω cm^2) that are somewhat smaller than those derived from the spectrum in Figure 7a.

We can assume that the resistance of the membrane is a result of the presence of pores spanning the bilayer thickness precisely, which are filled with the electrolyte solution. Making this assumption, we can calculate the relative pore area fraction by the following equation:

$$R_m/A_e = r_o L/A_p \tag{1}$$

where L is the length of the pore of the membrane (5 nm), A_p is the pore area, A_e is the area of the electrode, and r_o is the resistivity of the electrolyte solution (16.67 Ω cm).[17] Then

Table 2. Best-Fit Parameters Derived from Experimental Impedance Spectra in Figure 7 and a Theoretical Impedance According to the Equivalent Circuit in Figure 6b

system	R_e, Ω cm^2	Y_O, F cm^{-2} s^{n-1}	n	R_f, Ω cm^2	C_m, F cm^{-2}	R_m, Ω cm^2
11L cushion/membrane (30:70 DOPC:DOPS)	32.02	2.27×10^{-5}	0.91	4.91×10^5	1.06×10^{-5}	1.89×10^7
11L cushion/membrane (20:50:30 DOPC:DOPS:Chol)	29.27	1.87×10^{-5}	0.93	4.90×10^5	1.38×10^{-5}	7.69×10^6

$$A_p/A_e = r_oL/R_m = 16.67\ \Omega\ cm \cdot 5 \times 10^{-7}\ cm/2 \times 10^7\ \Omega$$

$$cm^2 \approx 4 \times 10^{-13}$$

A pore area fraction of 4×10^{-13} of the total electrode area is indicative of a very dense membrane, as one would expect from the calculated resistance. It is the first time that a dense lipid membrane, with resistance comparable with that of black membranes, has been achieved on polyelectrolyte multilayers, and to our knowledge none of the works on membranes supported on polymer cushions show these high resistance values for the supported membranes.

The reason why such resistance values have not been achieved before could be attributed to the use of lipid mixtures and assembly conditions that do not lead to a lipid bilayer on polyelectrolyte multilayers but lead to the assembly of, at least partially, vesicles that do not fully fuse. This ultimately affects the homogeneity of the lipid bilayer on the electrode surface and might induce pores or defects.

A logical step after achieving such dense membranes would be to incorporate channels or transmembrane proteins to increase selective passage of ions, which could have applications in the development of electrochemical sensors. A dense lipid membrane on top of a hydrophilic cushion as a spacer from the electrode is of fundamental interest as it would allow the study of the electrochemical properties of ion channels and transmembrane proteins, avoiding the direct contact of the molecules with the electrode and reducing the impact of the electrode on the channels or the biomolecules.

Impedance spectra shown in Figure 8 were measured with electrodes modified as described for Figure 7a with further
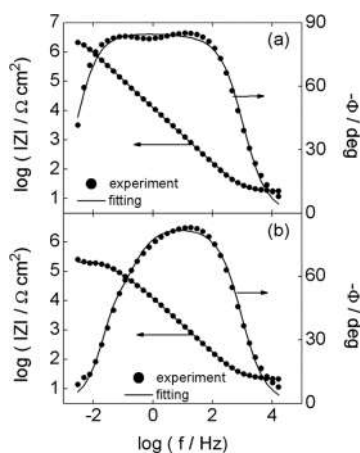
Figure 8. Bode plots for impedance spectra of lipid bilayers supported on an 11-layer PE cushion with a composition of (a) 30:70 DOPC:DOPS with an extra assembled one-layer and (b) three-layer PE array on top. Experimental spectra were fitted to the impedance of the equivalent circuit in Figure 6b.

assembly of one (Figure 8a) and three (Figure 8b) PE layers on top of the lipid layers. The experimental spectra can be successfully fitted to the impedance of the equivalent circuit in Figure 6b and resemble qualitatively those obtained with supported lipid bilayers doped with ionophores. The two time constants for the two RC networks (R_fQ_f and R_mC_m) result in an inflection point of the phase angle vs log f plot that can be detected for a frequency range at which the transition between these two regimes takes place.

Best-fit results of impedance data in Figure 8 are given in Table 3. A lipid bilayer confined in a sandwich structure between two PE films results in a decrease in R_m values and increase in C_m values, as compared with the system of Figure 8a. Moreover, R_f is also smaller in the presence of a film with three layers of PE on top of the bilayer, as compared with a capping film of only one layer of PE. Additionally, the capacitance (see Y_O values) of the PE film in the water subphase also decreases in the presence of three capping layers as compared with a one capping layer film. This is the reason why at each frequency the maximum of the phase shift for the relaxation processes due to the underlying PE film exhibits lower values in the former case, although separation between the two maxima remains constant. Again, impedance data in Figure 8 resembles the response measured for a lipid bilayer containing lipid-soluble ion transporters or, equivalently, numerous ion channels. This suggests that the lipid−PE interaction in the present sandwich-like configuration enhances ion transport through the bilayer.

Charge imbalance across the bilayer,[37] lateral tension for the lipid mobility,[38] and mechanical stress[39] may cause the presence of pores in protein-free phospholipid membranes. The polyelectrolyte deposited on top of the lipid layers can induce rearrangement of the lipids underneath. DOPS lipids will tend to complex the charged amine groups of PAH, inducing a redistribution of the lipids and probably generating some free space in the lipid layers as the negative charged lipids will accumulate in the areas where PAH is assembled. The assembly of PSS can also alter the lipid distribution, repulsing the charged lipids but interacting with the quaternary amines of DOPC.[40] For three polyelectrolyte layers there is large interdigitation and it is likely that the third layer of PAH alters again the lipid distribution pattern. Our results show that three layers on top of the bilayer are more effective in increasing layer conductance, which can be interpreted as a consequence of the formation of a layer with more defects or pores. In conclusion, the PE−lipid membrane interactions enable pore-mediated transport of ionic species across a lipid membrane. Capacitance is however only slightly affected by the assembly of the PEMs. The values of capacitance increase approximately 3 times after the polyelectrolyte assembly. The polyelectrolyte assembly on top of the bilayer seems to favor the high capacitance values, probably due to the electrostatic interaction between the lipids and the polyelectrolytes or because there is more interdigitation between lipids when both lipid monolayers are facing polyelectrolyte. In any case, the high capacitance indicate that although more defects are formed in the bilayer, increasing conductivity, the bilayer is not losing connectivity and

Table 3. Best-Fit Parameters Derived from Experimental Impedance Spectra in Figure 8 and Theoretical Impedance According to the Equivalent Circuit in Figure 6b

system	R_e, Ω cm^2	Y_O, F cm^{-2} s^{n-1}	n	R_f, Ω cm^2	C_m, F cm^{-2}	R_m, Ω cm^2
11L PE film/membrane (30:70 DOPC:DOPS)/1L PE film	18.36	2.52×10^{-5}	0.9	1.87×10^6	3.17×10^{-5}	1.62×10^6
11L PE film/membrane (30:70 DOPC:DOPS)/3L PE film	22.1	2.32×10^{-5}	0.89	4.82×10^4	3.65×10^{-5}	1.64×10^5

continues acting as a capacitor. This would mean that the polyelectrolyte deposition only induces small defects in the bilayer in agreement with Pilbat et al.,[41] who observe that polyelectrolytes assembled on top of lipid layers deposited on PEMs do not get in contact with the supporting PEM and they do not cross the lipid layers.

CONCLUSIONS

EIS measurements show for the first time that a lipid bilayer deposited on top of a polyelectrolyte multilayer cushion can attain high resistance values, 1.89×10^7 Ω cm^2. This high resistance results from the formation of a dense lipid bilayer with a limited number of defects or pores ($\sim 10^{-11}$% of the total area). Previous works on lipid bilayers deposited on top of poyelectrolyte multilayes did not show such dense membranes, and the resistance for the lipid bilayers was significantly lower. The lipid composition of the vesicles used for lipid assembly ensures the formation of a continuous bilayer on top of the PAH/PSS multilayers. Previous works on lipid bilayers on PEMs used other lipid compositions for the vesicles, which might lead to incomplete fusion of the lipids into a bilayer or even the assembly of nonfused vesicles. A continuous bilayer exhibits fewer pores or defects than an assembly of nonfused vesicles, explaining the high resistance values measured by EIS.

The capacitance of the lipid bilayer is however larger than for other dense supported membranes. This is most likely a result of the lipid composition and the interaction of the lipids with the polyelectrolytes causing changes in the dielectric constant on the lipid side in contact with the polyelectrolyte and a redistribution of the charged lipids toward the lipid layer in contact with the PE. The assembly of PE on top of the lipids results in the formation of pores or defects in the lipid layer with a subsequent decrease in the resistance of up to 2 orders of magnitude. These results show the influence of the polyelectrolytes on the lipid arrangement in the bilayers, generating regions of different density of charged and zwitterionic lipids.

Our results open new perspectives on the use of lipid bilayers on supported polymer cushions. The high resistance obtained here envisages the combination of lipid layers with channels or transmembrane proteins for selective transport in devices or as model for biological processes, taking advantage of the use of polyelectrolyte multilayers as hydrophilic spacers.

ASSOCIATED CONTENT

Ⓢ Supporting Information

The Supporting Information is available free of charge on the ACS Publications website at DOI: 10.1021/acs.langmuir.6b01191.

Details of electrochemical impedance and control experiments (PDF)

AUTHOR INFORMATION

Corresponding Authors
*E-mail: smoya@cicbimagune.es (S.E.M.).
*E-mail: gervasi@inifta.unlp.edu.ar (C.A.G.).
*E-mail: azzaroni@inifta.unlp.edu.ar (O.A.).

Notes
The authors declare no competing financial interest.

REFERENCES

(1) Keller, C. A.; Kasemo, B. Surface Specific Kinetics of Lipid Vesicle Adsorption Measured with a Quartz Crystal Microbalance. *Biophys. J.* **1998**, *75* (3), 1397−1402.

(2) Reimhult, E.; Höök, F.; Kasemo, B. Vesicle Adsorption on SiO[sub 2] and TiO[sub 2]: Dependence on Vesicle Size. *J. Chem. Phys.* **2002**, *117* (16), 7401.

(3) Reimhult, E.; Zäch, M.; Höök, F.; Kasemo, B. A Multitechnique Study of Liposome Adsorption on Au and Lipid Bilayer Formation on SiO2. *Langmuir* **2006**, *22* (7), 3313−3319.

(4) Cremer, P. S.; Boxer, S. G. Formation and Spreading of Lipid Bilayers on Planar Glass Supports. *J. Phys. Chem. B* **1999**, *103*, 2554−2559.

(5) Spinke, J.; Yang, J.; Wolf, H.; Liley, M.; Ringsdorf, H.; Knoll, W. Polymer-Supported Bilayer on a Solid Substrate. *Biophys. J.* **1992**, *63* (6), 1667−1671.

(6) McConnell, H. M.; Watts, T. H.; Weis, R. M.; Brian, A. A. Supported Planar Membranes in Studies of Cell-Cell Recognition in the Immune System. *Biochim. Biophys. Acta, Rev. Biomembr.* **1986**, *864* (1), 95−106.

(7) Vallejo, A. E.; Gervasi, C. A. Chapter 10 On the Use of Impedance Spectroscopy for Studying Bilayer Lipid Membranes. *Adv. Planar Lipid Bilayers Liposomes* **2006**, *3*, 331−353.

(8) Naumowicz, M.; Figaszewski, Z. Impedance Analysis of Phosphatidylcholine Membranes Modified with Gramicidin D. *Bioelectrochemistry* **2003**, *61* (1−2), 21−27.

(9) Terrettaz, S.; Mayer, M.; Vogel, H. Highly Electrically Insulating Tethered Lipid Bilayers for Probing the Function of Ion Channel Proteins. *Langmuir* **2003**, *19* (14), 5567−5569.

(10) Wiegand, G.; Arribas-Layton, N.; Hillebrandt, H.; Sackmann, E.; Wagner, P. Electrical Properties of Supported Lipid Bilayer Membranes. *J. Phys. Chem. B* **2002**, *106* (16), 4245−4254.

(11) Tanaka, M.; Sackmann, E. Polymer-Supported Membranes as Models of the Cell Surface. *Nature* **2005**, *437* (7059), 656−663.

(12) Chanana, M.; Gliozzi, A.; Diaspro, A.; Chodnevskaja, I.; Huewel, S.; Moskalenko, V.; Ulrichs, K.; Galla, H.-J.; Krol, S. Interaction of Polyelectrolytes and Their Composites with Living Cells. *Nano Lett.* **2005**, *5* (12), 2605−2612.

(13) Reimhult, E.; Kasemo, B.; Höök, F. Rupture Pathway of Phosphatidylcholine Liposomes on Silicon Dioxide. *Int. J. Mol. Sci.* **2009**, *10* (4), 1683−1696.

(14) Edvardsson, M.; Svedhem, S.; Wang, G.; Richter, R.; Rodahl, M.; Kasemo, B. QCM-D and Reflectometry Instrument: Applications to Supported Lipid Structures and Their Biomolecular Interactions. *Anal. Chem.* **2009**, *81* (1), 349−361.

(15) Rossetti, F. F.; Textor, M.; Reviakine, I. Asymmetric Distribution of Phosphatidyl Serine in Supported Phospholipid Bilayers on Titanium Dioxide. *Langmuir* **2006**, *22* (8), 3467−3473.

(16) Naumann, R.; Schiller, S. M.; Giess, F.; Grohe, B.; Hartman, K. B.; Kärcher, I.; Köper, I.; Lübben, J.; Vasilev, K.; Knoll, W. Tethered Lipid Bilayers on Ultraflat Gold Surfaces. *Langmuir* **2003**, *19* (13), 5435−5443.

(17) Cassier, T.; Sinner, A.; Offenhäuser, A.; Möhwald, H. Homogeneity, Electrical Resistivity and Lateral Diffusion of Lipid

Bilayers Coupled to Polyelectrolyte Multilayers. *Colloids Surf., B* **1999**, *15* (3–4), 215–225.

(18) Decher, G.; Hong, J. D.; Schmitt, J. Buildup of Ultrathin Multilayer Films by a Self-Assembly Process: III. Consecutively Alternating Adsorption of Anionic and Cationic Polyelectrolytes on Charged Surfaces. *Thin Solid Films* **1992**, *210–211*, 831–835.

(19) Decher, G.; Eckle, M.; Schmitt, J.; Struth, B. Layer-by-Layer Assembled Multicomposite Films. *Curr. Opin. Colloid Interface Sci.* **1998**, *3* (1), 32–39.

(20) Moya, S.; Donath, E.; Sukhorukov, G. B.; Auch, M.; Baumler, H.; Lichtenfeld, H.; Mohwald, H. Lipid Coating on Polyelectrolyte Surface Modified Colloidal Particles and Polyelectrolyte Capsules. *Macromolecules* **2000**, *33*, 4538–4544.

(21) Georgieva, R.; Moya, S.; Leporatti, S.; Neu, B.; Baumler, H.; Reichle, C.; Donath, E.; Mohwald, H. Conductance and Capacitance of Polyelectrolyte and Lipid-Polyelectrolyte Composite Capsules As Measured by Electrorotation. *Langmuir* **2000**, *16* (17), 7075–7081.

(22) Georgieva, R.; Moya, S. E.; Bäumler, H.; Möhwald, H.; Donath, E. Controlling Ionic Conductivity in Lipid Polyelectrolyte Composite Capsules by Cholesterol. *J. Phys. Chem. B* **2005**, *109* (38), 18025–18030.

(23) Fischlechner, M.; Zaulig, M.; Meyer, S.; Estrela-Lopis, I.; Cuéllar, L.; Irigoyen, J.; Pescador, P.; Brumen, M.; Messner, P.; Moya, S.; et al. Lipid Layers on Polyelectrolyte Multilayer Supports. *Soft Matter* **2008**, *4* (11), 2245.

(24) Kügler, R.; Knoll, W. Polyelectrolyte-Supported Lipid Membranes. *Bioelectrochemistry* **2002**, *56* (1–2), 175–178.

(25) Jenkins, A. T. A.; Bushby, R. J.; Boden, N.; Evans, S. D.; Knowles, P. F.; Liu, Q.; Miles, R. E.; Ogier, S. D. Ion-Selective Lipid Bilayers Tethered to Microcontact Printed Self-Assembled Monolayers Containing Cholesterol Derivatives. *Langmuir* **1998**, *14* (17), 4675–4678.

(26) Singh, S.; Junghans, A.; Tian, J.; Dubey, M.; Gnanakaran, S.; Chlistunoff, J.; Majewski, J. Polyelectrolyte Multilayers as a Platform for pH-Responsive Lipid Bilayers. *Soft Matter* **2013**, *9* (37), 8938.

(27) Benz, R.; Janko, K. Voltage-Induced Capacitance Relaxation of Lipid Bilayer Membranes Effects of Membrane Composition. *Biochim. Biophys. Acta, Biomembr.* **1976**, *455* (3), 721–738.

(28) Alonso-Romanowski, S.; Gassa, L. M.; Vilche, J. R. An Investigation by EIS of Gramicidin Channels in Bilayer Lipid Membranes. *Electrochim. Acta* **1995**, *40* (10), 1561–1567.

(29) Ries, R. S.; Choi, H.; Blunck, R.; Bezanilla, F.; Heath, J. R. Black Lipid Membranes: Visualizing the Structure, Dynamics, and Substrate Dependence of Membranes. *J. Phys. Chem. B* **2004**, *108* (41), 16040–16049.

(30) Guidelli, R.; Becucci, L. Electrochemistry of Biomimetic Membranes. *Mod. Aspects Electrochem.* **2012**, *53*, 147–266.

(31) Lin, J.; Hristova, K.; Searson, P. Electrically Addressable, Biologically Relevant Surface-Supported Bilayers. In *Handbook of Biofunctional Surfaces*; Pan Stanford Publishing: 2013; pp 769–820.

(32) Stelzle, M.; Weissmuller, G.; Sackmann, E. On the Application of Supported Bilayers as Receptive Layers for Biosensors with Electrical Detection. *J. Phys. Chem.* **1993**, *97* (12), 2974–2981.

(33) Iturri Ramos, J. J.; Stahl, S.; Richter, R. P.; Moya, S. E. Water Content and Buildup of Poly(diallyldimethylammonium chloride)/Poly(sodium 4-Styrenesulfonate) and Poly(allylamine hydrochloride)/Poly(sodium 4-Styrenesulfonate) Polyelectrolyte Multilayers Studied by an in Situ Combination of a Quartz Crystal Microb. *Macromolecules* **2010**, *43* (21), 9063–9070.

(34) Läuger, P.; Lesslauer, W.; Marti, E.; Richter, J. Electrical Properties of Biomolecular Phospholipid Membranes. *Biochim. Biophys. Acta, Biomembr.* **1967**, *135*, 20–32.

(35) Janshoff, A.; Steinem, C. Supported Lipid Bilayers: Intelligent Surfaces for Ion Channel Recordings. In *Intelligent Surfaces in Biotechnology*; John Wiley & Sons, Inc.: Hoboken, NJ, USA, 2012; pp 141–182.

(36) Plant, A. L. Self-Assembled Phospholipid Alkanethiol Biomimetic Bilayers on Gold. *Langmuir* **1993**, *9* (11), 2764–2767.

(37) Gurtovenko, A. A.; Vattulainen, I. Pore Formation Coupled to Ion Transport through Lipid Membranes as Induced by Transmembrane Ionic Charge Imbalance: Atomistic Molecular Dynamics Study. *J. Am. Chem. Soc.* **2005**, *127* (50), 17570–17571.

(38) Lin, J.; Szymanski, J.; Searson, P. C.; Hristova, K. Effect of a Polymer Cushion on the Electrical Properties and Stability of Surface-Supported Lipid Bilayers. *Langmuir* **2010**, *26* (5), 3544–3548.

(39) Leontiadou, H.; Mark, A. E.; Marrink, S. J. Molecular Dynamics Simulations of Hydrophilic Pores in Lipid Bilayers. *Biophys. J.* **2004**, *86* (4), 2156–2164.

(40) Diamanti, E.; Cuellar, L.; Gregurec, D.; Moya, S. E.; Donath, E. Role of Hydrogen Bonding and Polyanion Composition in the Formation of Lipid Bilayers on Top of Polyelectrolyte Multilayers. *Langmuir* **2015**, *31*, 8623–8632.

(41) Pilbat, A. M.; Szegletes, Z.; Kóta, Z.; Ball, V.; Schaaf, P.; Voegel, J. C.; Szalontai, B. Phospholipid Bilayers as Biomembrane-like Barriers in Layer-by-Layer Polyelectrolyte Films. *Langmuir* **2007**, *23* (15), 8236–8242.